Numerical calculations of the phase diagram of cubic blue phases in cholesteric liquid crystals

A. Dupuis, D. Marenduzzo, and J. M. Yeomans
The Rudolf Peierls Centre for Theoretical Physics, 1 Keble Road, Oxford OX1 3NP, United Kingdom
(Received 3 August 2004; published 20 January 2005)

We study the static properties of cubic blue phases by numerically minimizing the three-dimensional, Landau–de Gennes free energy for a cholesteric liquid crystal close to the isotropic-cholesteric phase transition. Thus we are able to refine the powerful but approximate, semianalytic frameworks that have been used previously. We obtain the equilibrium phase diagram and discuss it in relation to previous results. We find that the value of the chirality above which blue phases appear is shifted by 20% (toward experimentally more accessible regions) with respect to previous estimates. We also find that the region of stability of the O_5 structure—which has not been observed experimentally—shrinks, while that of blue phase I(O_8^-) increases thus giving the correct order of appearance of blue phases at small chirality. We also study the approach to equilibrium starting from the infinite chirality solutions and we find that in some cases the disclination network has to assemble during the equilibration. In these situations disclinations are formed via the merging of isolated aligned defects.

DOI: 10.1103/PhysRevE.71.011703 PACS number(s): 61.30.Mp, 83.80.Xz, 61.30.Dk

I. INTRODUCTION

Liquid crystals are typically composed of highly anisotropic molecules. They are viscoelastic materials; some of their properties are typical of a liquid while others are usually associated with solids. As liquids, they can flow and they exhibit a viscous response to an applied stress. However, liquid crystals also possess long-range, orientational order [1,2] which results from the entropic advantage of aligning the constituent molecules. The long-range, orientational order is usefully described by the director field $\vec{n}$, the coarse-grained, average, molecular orientation. In a cholesteric or chiral nematic liquid crystal $\vec{n}$ has a natural twist deformation along an axis perpendicular to the molecules [1,2]. Examples of cholesteric liquid crystals are DNA molecules in solution, colloidal suspensions of bacteriophages [3], and solutions of nematic mixtures with chiral dopants which are widely used in display devices.

A particularly intriguing phase of liquid crystals is obtained by slowly cooling down a liquid crystal from the isotropic into the cholesteric phase. Instead of a direct transition into a helical configuration, it was found experimentally that the system passes through a series of first-order phase transitions, all of which occur in a temperature range of roughly 1 K [4,5]. These phases are known as blue phases. Typically [4], experiments report a series of at least three phases intervening in this small temperature range. The series of transitions is often as follows: isotropic (I)→blue phase III (BP III)→blue phase II (BP II)→blue phase I (BP I)→cholesteric (C). BP I and BP II display a cubic symmetry, while BP III has an amorphous nature. Blue phases are now beginning to find applications in lasers [6] and in electric field driven devices [7].

Blue phases provide a particularly fascinating example of liquid crystal ordering as they correspond to complicated director fields which, even in equilibrium, are threaded by a regular network of disclinations [8–13]. Identifying their structure presented a considerable theoretical challenge the resolution of which is clearly summarized in the review by Wright and Mermin [4].

In the literature attention has mainly focused on four different candidates for the cubic blue phases. The nomenclature used here refers to the symmetry group which characterizes the lattice of disclinations formed in the blue phases following [4,11,12]. O_2 has the symmetry of a simple cubic lattice, $O_8^{+,-}$ and O_5 that of a body-centered-cubic lattice. The two O_8 phases are candidates for BP I as they have the same octahedral symmetry, while O_2 has been proposed as a model for BP II. The defect structure in each phase in shown in Fig. 1. In O_2 and in O_5 the defect lines merge in the center of the

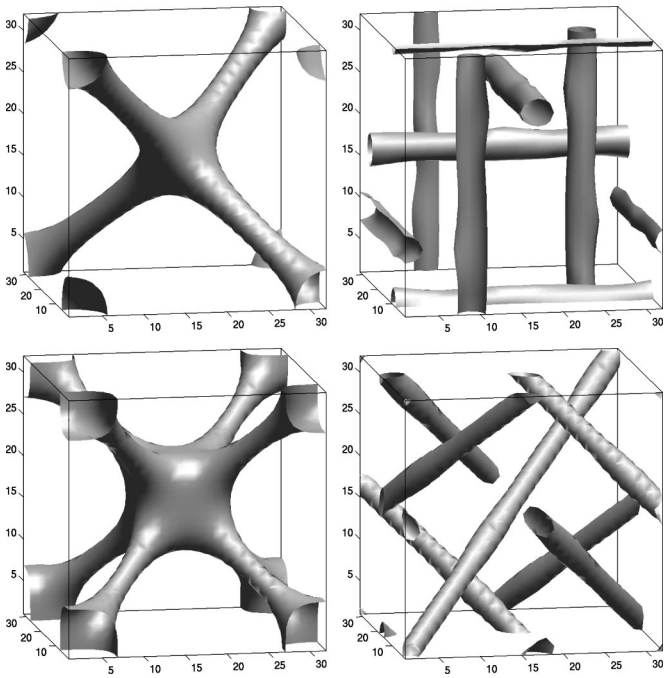

FIG. 1. Defect structure where $\gamma=2.80$ and $A_0=0.001$ for (top left) O_2, (bottom left) O_5, (top right) O_8^+, and (bottom right) O_8^-.

unit cell, whereas in the octahedral phases the defects avoid each other.

The **Q** tensor theory, in which the local conformation of the liquid crystal is specified by a tensor, and not only by the director field $\vec{n}$, is the natural language to understand the equilibrium properties of blue phases because it is able to capture their inherent biaxiality [4]. With the advent of more powerful computers it is now possible to numerically minimize the free energy for any value of the chirality κ without further approximation than that inherent in the free energy expression itself. This is the program we follow in this paper.

We determine the equilibrium phase diagram which specifies which of the cubic blue phases has the lowest free energy as a function of the system parameters. We find a phase diagram qualitatively similar to that found in earlier work and compatible with the assignments BP I $=O_8^-$ and BP II $=O_2$. However, there are quantitative differences. In particular the results show that the triple point between the cholesteric and blue phases is lowered in chirality by around 20%. We also show that the region of stability of O_5 shrinks and that of O_8^- increases with respect to the previous estimates. The revised phase diagram is more compatible with observations suggesting that the Landau–de Gennes theory is sufficient to explain the static observations on blue phases. Finally, we characterize the approach to equilibrium and in particular we describe the dynamic pathway by which the disclination structure of O_8^- assembles in the simulations.

II. LANDAU–de GENNES THEORY FOR CHOLESTERIC BLUE PHASES

The equilibrium properties of the liquid crystal are described by a Landau–de Gennes free energy density expanded in terms of a tensor order parameter **Q**. This is related to the direction of individual molecules, $\hat{n}$, by $Q_{\alpha\beta}=\langle \hat{n}_\alpha \hat{n}_\beta - \frac{1}{3}\delta_{\alpha\beta}\rangle$ where the angular brackets denote a coarse-grained average and the Greek indices label the Cartesian components of **Q**. The tensor **Q** is traceless and symmetric. Its largest eigenvalue, $\frac{2}{3}q$, $0<q<1$, describes the magnitude of the order.

The free energy comprises a bulk term $\mathcal{F}_b$ (summation over repeated indices is implied hereafter in our notation)

$$\mathcal{F}_b = \frac{A_0}{2}\left(1-\frac{\gamma}{3}\right)Q_{\alpha\beta}^2 - \frac{A_0\gamma}{3}Q_{\alpha\beta}Q_{\beta\gamma}Q_{\gamma\alpha} + \frac{A_0\gamma}{4}(Q_{\alpha\beta}^2)^2 \tag{1}$$

and a distortion term, $\mathcal{F}_d$, which for cholesterics is [1,4]

$$\mathcal{F}_d = \frac{K}{2}[(\partial_\beta Q_{\alpha\beta})^2 + (\epsilon_{\alpha\zeta\delta}\partial_\zeta Q_{\delta\beta} + 2q_0 Q_{\alpha\beta})^2], \tag{2}$$

where K is an elastic constant and $q_0=2\pi/p$, with p the pitch of the cholesteric liquid crystal. The tensor $\epsilon_{\alpha\zeta\delta}$ is the Levi–Civita antisymmetric third-rank tensor, A_0 is a constant and γ controls the magnitude of the order (physically it corresponds to an effective temperature or concentration for thermotropic and lyotropic liquid crystal, respectively). This free energy has the same functional form of the one employed in Refs. [9,10], but the latter is more general as it contains one more parameter in the bulk free energy density term.

Of particular interest for the present discussion of blue phase equilibrium [4] are two quantities, the chirality κ, and the reduced temperature τ. These are defined in Ref. [10] and in our formulation they can be found via

$$\kappa = \sqrt{\frac{108Kq_0^2}{A_0\gamma}},$$

$$\tau = \frac{27A_0(1-\gamma/3)+108Kq_0^2}{A_0\gamma} = \frac{27(1-\gamma/3)}{\gamma}+\kappa^2. \tag{3}$$

Approaches to study the equilibrium properties of blue phases which have given a great deal of insight into the phase behavior have so far been based on an expansion in the parameter κ. *High chirality* theories are strictly valid for infinite κ. In that case an infinite number of exact minimizers of the free energy density can be found as an arbitrary sum of biaxial helices [4]. *Low chirality* theories have also been formulated. These rely on the Frank free energy defined in terms of the coarse grained director field $\vec{n}$ instead of **Q**: this is equivalent to assuming a uniaxial order parameter.

In this work we do not make assumptions about the value of κ but rather minimize the Landau–de Gennes free energy by numerically solving an equation of motion for **Q** [14]

$$\frac{\partial Q_{\alpha\beta}}{\partial t} = \Gamma H_{\alpha\beta}, \tag{4}$$

where Γ is a collective rotational diffusion constant.

The term on the right-hand side of Eq. (4) describes the relaxation of the order parameter toward the minimum of the free energy. The molecular field **H** which provides the driving force is related to the derivative of the free energy $\mathcal{F}$ by

$$\mathbf{H} = -\frac{\delta\mathcal{F}}{\delta\mathbf{Q}} + (\mathbf{I}/3)\mathrm{Tr}\frac{\delta\mathcal{F}}{\delta\mathbf{Q}}, \tag{5}$$

where Tr denotes the tensorial trace. From Eqs. (1) and (2), the molecular field is explicitly

$$H_{\alpha\beta} = (A_0(1-\gamma/3)+4Kq_0^2)Q_{\alpha\beta} - A_0\gamma\left(Q_{\alpha\gamma}Q_{\gamma\beta} - \frac{\delta_{\alpha\beta}}{3}Q_{\gamma\delta}^2\right) + A_0\gamma Q_{\gamma\delta}^2 Q_{\alpha\beta} + K\partial_\gamma^2 Q_{\alpha\beta} - 4Kq_0\epsilon_{\alpha\gamma\delta}\partial_\gamma Q_{\delta\beta}. \tag{6}$$

III. NUMERICAL ALGORITHM

Our aim in this work is to numerically minimize—by solving Eq. (4) using a lattice Boltzmann algorithm—the free energies of the cubic blue phases O_2, O_5, O_8^+, and O_8^-. In this section we report the procedure used.

The equilibrium state for chosen values of chirality κ and reduced temperature τ was obtained as the steady-state solution of the equation of motion (4). The initial condition for each phase was taken as its configuration for infinite chirality ($\kappa=\infty$ or $A_0=0$) for which exact analytical expressions are available [4]. In the $\kappa=\infty$ limit the **Q** tensors characterizing the blue phases retain the correct topology of the disclination lines. As expected this was preserved under the dynamics

allowing us to minimize the free energy for a structure with the chosen network of disclinations for any value of τ and κ.

For completeness we report here the initial configurations chosen in this work. (Note that in all cases the components *yy*, *zz*, *xz*, and *yz* are obtained by cyclic permutation from those given below.)

The initial configuration for O_2 is

$$Q_{xx} = A\{\cos(2q_0 z) - \cos(2q_0 y)\}, \quad Q_{xy} = -A\sin(2q_0 z), \tag{7}$$

where $A>0$ is an arbitrary amplitude.

That for O_5 is

$$Q_{xx} = A\{2\cos(\sqrt{2}q_0 y)\cos(\sqrt{2}q_0 z) - \cos(\sqrt{2}q_0 x)\cos(\sqrt{2}q_0 z) - \cos(\sqrt{2}q_0 x)\cos(\sqrt{2}q_0 y)\}, \tag{8}$$

$$Q_{xy} = A\{\sqrt{2}\cos(\sqrt{2}q_0 y)\sin(\sqrt{2}q_0 z) - \sqrt{2}\cos(\sqrt{2}q_0 x)\sin(\sqrt{2}q_0 z) - \sin(\sqrt{2}q_0 x)\sin(\sqrt{2}q_0 y)\},$$

where $A>0$.

Those for $O_8^{+,-}$ are

$$Q_{xx} = A\{-2\cos(\sqrt{2}q_0 y)\sin(\sqrt{2}q_0 z) + \sin(\sqrt{2}q_0 x)\cos(\sqrt{2}q_0 z) + \cos(\sqrt{2}q_0 x)\sin(\sqrt{2}q_0 y)\}, \tag{9}$$

$$Q_{xy} = A\{\sqrt{2}\cos(\sqrt{2}q_0 y)\cos(\sqrt{2}q_0 z) + \sqrt{2}\sin(\sqrt{2}q_0 x)\sin(\sqrt{2}q_0 z) - \sin(\sqrt{2}q_0 x)\cos(\sqrt{2}q_0 y)\},$$

where A is positive for O_8^+ and negative for O_8^-.

In general, the minimum free energy for blue phases is not attained when the periodicity of the disclination lattice matches the pitch of the cholesteric helix p but when the unit cell is larger. This is accounted for by considering alternative initial conditions with q_0 substituted by rq_0 [8–10], with $r<1$. Since the lattice periodicity is bigger than that for the infinite chirality solutions, r is referred to as a "redshift." We checked the validity of the values of r suggested in Ref. [10] and then used them to build the initial conditions. If redshift is not accounted for, the region of stability of blue phases does not change significantly, but the O_8^- phase is not found.

Details of the lattice Boltzmann algorithm used to solve the equation of motion are given in Refs. [15–17]. Calculations were performed on a parallel machine, for a $32\times32\times32$ cubic lattice. This means that, for example, in the case of O_2 a cholesteric pitch was discretized into 64 lattice points. Typically, the simulation of one point in the phase space (κ,τ) ran on eight processors and required 8 hours of computational time. Periodic boundary conditions were used throughout. To ensure that equilibrium was reached, we required that the variation in the free energy after 200 iterations of Eq. (4) was smaller than 10^{-4} before ending the run. A convenient value of Γ, ensuring numerical stability and fast computation time, was 0.33775.

The parameters defining the free energy were chosen to match typical values for cholesterics. In what follows the points on the phase diagram will be labeled by their (κ,τ) (as in Ref. [10]) or (A_0,γ) values. These can be related straightforwardly via the transformation in Eq. (3).

IV. RESULTS

In this section we report the results obtained for the defect structure of the blue phases, and the equilibrium phase diagram in the vicinity of the isotropic-cholesteric transition. We also consider the dynamics of the defect lines as equilibrium is approached.

A. Defect structure: O_2, O_5, O_8^+, and O_8^-

As a first check, we compute the defect structure associated with the cubic blue phases after equilibration. We choose $A_0=0.001$ and $\gamma=2.8$, while the elastic constant $K=0.01$ for O_2, and $K=0.005$ for O_5 and $O_8^{+,-}$. These correspond to a chirality $\kappa=1.93$ and a reduced temperature $\tau=4.37$. The resulting disclination line networks are shown in Fig. 1. The tubes in the figure represent regions of the blue phase unit cell in which the order parameter drops below some specified threshold, i.e., they represent disclination lines. The thickness of the tubes is related to the width of the defect cores.

These structures are in good agreement with those obtained in Refs. [10–12]. We note that the structure of the defects depends on the parameters. If A_0 or γ are increased, i.e., if κ decreases, then the width of the disclinations decreases and the drop in order parameter at the defect cores becomes shallower.

We also checked the three-dimensional director field profile and found the presence of distinct regions of double twist separated by the defects shown in Fig. 1, in qualitative agreement with the usual theoretical picture of blue phases [9,10,13].

B. Phase diagram

Next we report results for the free energy of the equilibrated blue phases. In Fig. 2 we show free energy curves for O_2, O_5, O_8^+, O_8^- and the isotropic and cholesteric phases for $A_0=0.001$ and variable γ. It can be seen that blue phases appear near the transition to the isotropic phase. As A_0 increases, the region of stability of blue phases shrinks. This is in agreement with previous experimental and analytical results in the literature [5,10–12].

In Fig. 3, we show the phase diagram in the (κ,τ) plane which identifies for every point which of the phases, O_2,O_5, $O_8^{+,-}$, cholesteric or isotropic, has the minimum free energy. For comparison we show, in the same plane, the phase diagram obtained in Ref. [10] which employed a Fourier expansion of the tensor-order parameter $\mathbf{Q}$ around the $\kappa=\infty$ limit. We stress that the main difference is that in our case we relax the structures (with the disclination network topology suggested in Ref. [10]) by dynamically solving Eq. (4). So the configurations used to construct our phase diagram are actual (in general local) minima of the Landau–de Gennes free en-

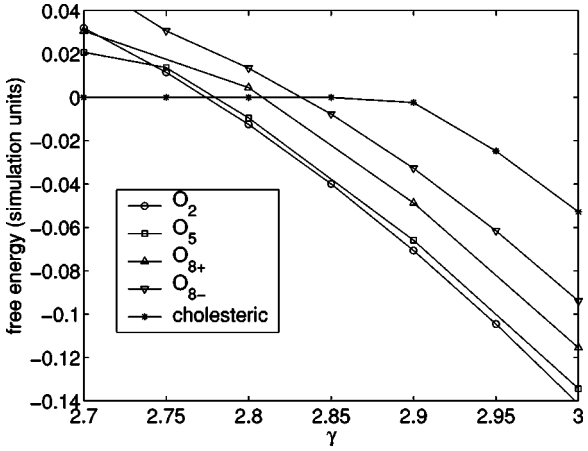

FIG. 2. Free energy of O_2, O_5, O_8^+, O_8^- and the cholesteric helix as a function of γ for $A_0=0.001$.

ergy. In Ref. [10], the configurations found correspond to the free energy minima within a restricted phase space in which the **Q** tensor expression is constrained to be a sum of spherical harmonics of order $m \leqslant 2$ with variable coefficients.

Overall, we find qualitative agreement in that (a) the stable phases found (for the parameters investigated here) are O_2, O_5, and O_8^-, (b) O_5 appears for high chirality only, and

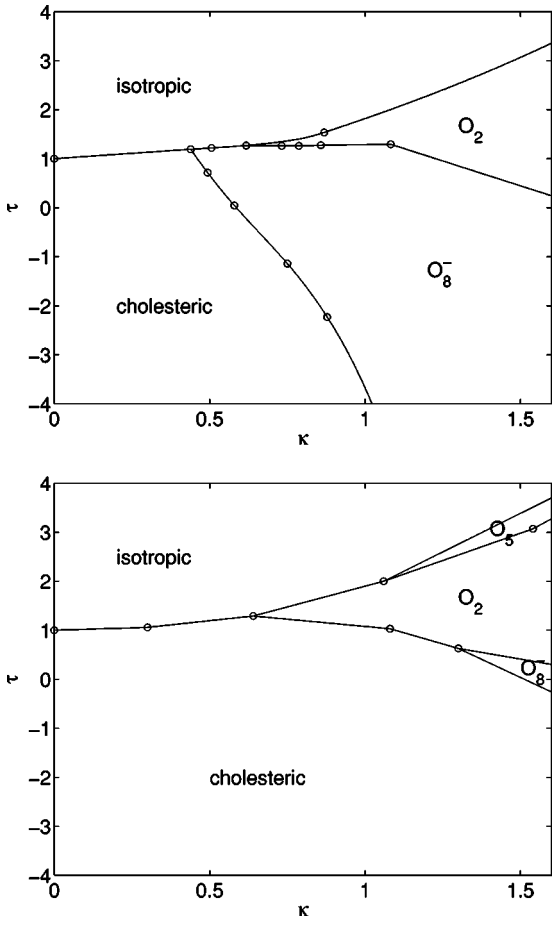

FIG. 3. Top: phase diagram in the (κ, τ) plane obtained numerically (this work). Bottom: phase diagram from Ref. [10].

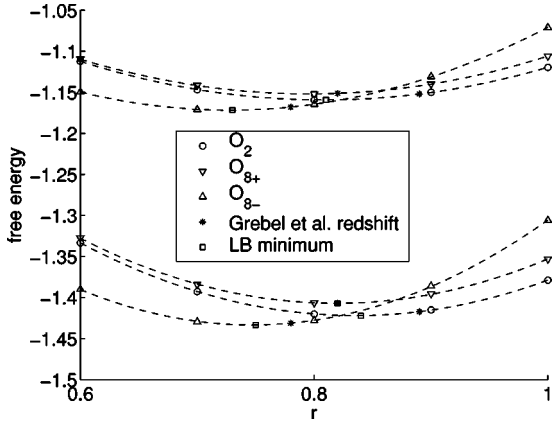

FIG. 4. Plot of the free energies (simulation units) versus r of O_2,O_8^+,O_8^- for two points in the (A_0, γ) plane [(0.006,3) for the top three curves and (0.002,3.5) for the bottom three]. Dashed lines are quadratic fits. Squares and stars show the numerical minimum and the one found in Grebel *et al.* [10], respectively.

(c) the phase diagram is consistent with the assignment of BP I as O_8^- and of BP II as O_2 proposed in [10,12]. However, a few relevant differences should be stressed. First, the region of stability of O_5 is shifted to unphysically high values of the chirality $\gtrsim 2$. (Values of $\kappa \lesssim 1.2$ are found in cholesterics.) This result is consistent with the observations, which ruled out structures of O_5 symmetry from the known blue phases. The region of stability of O_8^- expands and reaches lower chirality values. The critical point below which blue phases are no longer stable is also shifted from $\kappa \sim 0.6$ to below $\kappa = 0.5$ (deeper into the experimentally accessible region). Pleasingly, this leads to the correct order of appearance of BP I and BP II as the chirality is increased (as found in the experiments). This was not achieved before within the Landau–de Gennes framework.

To construct the phase diagram in Fig. 3, we used the values of the redshift from Ref. [10], which were obtained within the approximate framework detailed above. As a check, for a few points in the phase diagram, we equilibrated systems with different redshifts. Plots of free energy versus redshifts for two points in the phase diagram are shown in Fig. 4. At all points we tested we found that the redshift values in Ref. [10] corresponded very closely to the free energy minimum. In this way we feel confident that an extensive calculation taking into account all possible redshifts for all data points, which is numerically extremely expensive, would give a quantitatively very similar phase diagram.

The discrepancy between the phase diagram obtained here and the one given in Ref. [10] show that high-order Fourier components of **Q** are important at least in some regions of the phase diagram. Indeed the authors of Ref. [10] noted that in a large part of the region where the phase diagrams differ the energies of the various phases are very close. Thus considering a larger variational space could well change the phase boundaries.

C. Dynamics of the approach to equilibrium

It is interesting to consider the dynamics of the approach to equilibrium of the blue phases from the infinite chirality

initial states. The O_2 and O_8^- structures are initially quite far from their equilibrium configurations, while the O_5 and O_8^+ configurations are closer. This means that the free energy for O_5 is lower than that of O_2 or O_8^- at the beginning of the simulations. During equilibration, the finite chirality deforms the tensor configurations of O_2 and O_8^- via a process which can be suggestively compared to the acquisition of an infinite number of harmonics in the language of [10] and the curves eventually cross. The approach to equilibrium of the free energy was in all cases found to be well represented by an exponential decay to the equilibrated value, with the decay rate playing the role of a relaxation time. Since the transitions are all (weakly) first order this is as expected on general grounds.

The most interesting dynamics of approach to equilibrium is that of O_8^-. In this case the initial structure does not closely resemble the equilibrium structure (see Fig. 5). In particular the disclination line along the axis [111] is only partially present. During equilibration, it assembles by the formation of isolated local defects aligned along [111] which then merge into a disclination line. The dynamical evolution was found to be almost independent of the values of $A_0 \neq 0$ and γ studied. It would be interesting to follow the evolution of the disclination line experimentally to see whether this effect can be realistic. Calculations are currently underway to check if the same pathway is followed when the full hydrodynamic equations of motion of the liquid crystal are solved.

V. CONCLUSIONS

In conclusion, we have numerically minimized the Landau–de Gennes free energy of a cholesteric liquid crystal and identified the region of stability of the blue phases. It was possible to obtain results for any values of the chirality κ, that is, for any degree of biaxiality of the tensor order parameter. Our results qualitatively confirm those obtained previously using expansions for large or small κ. However there are quantitative differences; in particular the blue phases first appear at a value of $\kappa \sim 20\%$ smaller than in the approximate minimizations. Also, it is interesting to note that the full numerical solution presented here produces the correct order of appearance of BP I and BP II at low chiralities, while the O_5 phase, which was not observed in experiments, is relegated to unphysical values of the chirality. We finally followed the approach to equilibrium. In the case of O_8^- the disclination network assembles during the equilibration via an intermediate state in which aligned isolated defects appear and then join to form the disclination line along the cube lattice diagonal.

Note that in two rather recent papers [18,19], it was found that adding fluctuations to the Landau–de Gennes free energy could render the phase diagram more realistic in that, e.g., the region of stability of O_5 was restricted. Here we find a similar result by an exact minimization of the mean field free energy without including fluctuations.

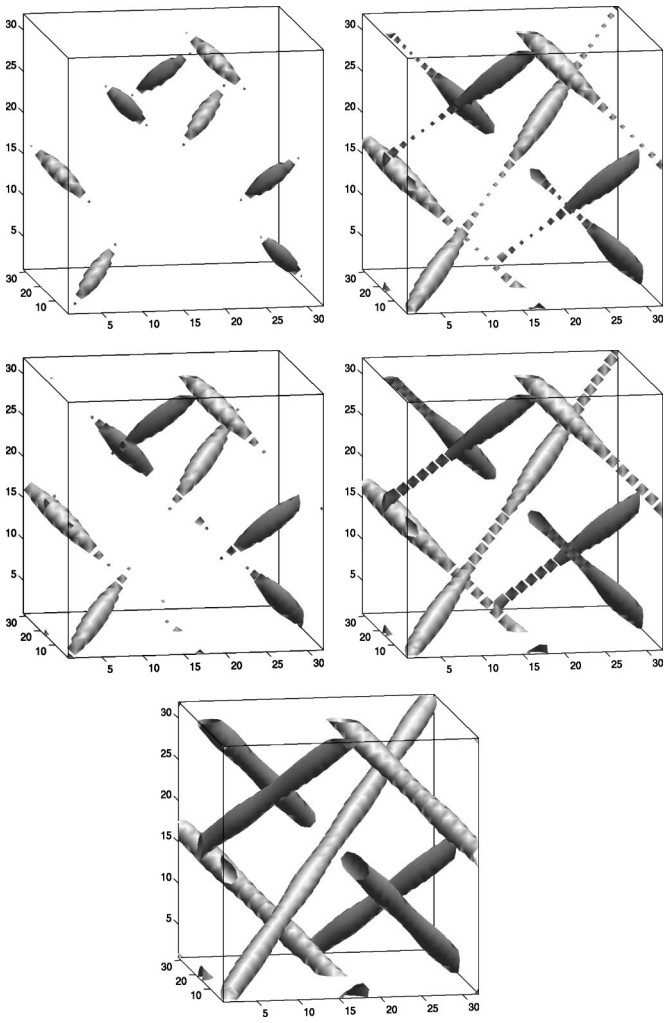

FIG. 5. Evolution of the defect structure (to be followed from left to right and top to bottom) for $\gamma=2.80$ and $A_0=0.001$, for the O_8^- configuration. The initial configuration is stable for $A_0=0$.

Finally, our approach can be generalized to study the effect of an electric field on the phase diagram as well as the dynamics of the switching of a blue phase device, such as the one proposed in Ref. [7]. Further work is underway along these lines.

ACKNOWLEDGMENTS

This work was supported by EPSRC Grant No. GR/R83712/01 and by EC IMAGE-IN project GRD1-CT-2002-00663. We thank the Oxford Supercomputing Centre and the Scientific and Parallel Computing group from the University of Geneva for providing supercomputing resources. We are grateful to E. Orlandini for many important discussions.

[1] P. G. de Gennes and J. Prost, *The Physics of Liquid Crystals*, 2nd ed. (Clarendon, Oxford, 1993).
[2] S. Chandrasekhar, *Liquid Crystals* (Cambridge University Press, Cambridge, U.K., 1980).
[3] E. Grelet and S. Fraden, Phys. Rev. Lett. **90**, 198302 (2003).
[4] D. C. Wright and N. D. Mermin, Rev. Mod. Phys. **61**, 385 (1989).
[5] M. Marcus and J. W. Goodby, Mol. Cryst. Liq. Cryst. Lett. **72**, 297 (1982).
[6] W. Y. Cao *et al.*, Nat. Mater. **1**, 111 (2002).
[7] H. Kikuchi *et al.*, Nat. Mater. **1**, 64 (2002).
[8] R. M. Hornreich and S. Shtrikman, Phys. Rev. A **24**, R635 (1981).
[9] H. Grebel, R. M. Hornreich, and S. Shtrikman, Phys. Rev. A **28**, 1114 (1983); **28**, 2544 (1983).
[10] H. Grebel, R. M. Hornreich, and S. Shtrikman, Phys. Rev. A **30**, 3264 (1984).
[11] S. Meiboom, M. Sammon, and W. F. Brinkmann, Phys. Rev. A **27**, 438 (1983).
[12] S. Meiboom, M. Sammon, and D. W. Berreman, Phys. Rev. A **28**, 3553 (1983).
[13] S. Meiboom, J. P. Sethna, P. W. Anderson, and W. F. Brinkman, Phys. Rev. Lett. **46**, 1216 (1981).
[14] A. N. Beris and B. J. Edwards, *Thermodynamics of Flowing Systems* (Oxford University Press, Oxford, 1994).
[15] C. Denniston, E. Orlandini, and J. M. Yeomans, Europhys. Lett. **52**, 481 (2000); Phys. Rev. E **63**, 056702 (2001).
[16] C. Denniston, D. Marenduzzo, E. Orlandini, and J. M. Yeomans, Philos. Trans. R. Soc. London, Ser. A **362**, 1745 (2004).
[17] D. Marenduzzo, E. Orlandini, and J. M. Yeomans, Phys. Rev. Lett. **92**, 188301 (2004).
[18] J. Englert, L. Longa, H. Stark, and H.-R. Trebin, Phys. Rev. Lett. **81**, 1457 (1998).
[19] J. Englert, H. Stark, L. Longa, and H.-R. Trebin, Phys. Rev. E **61**, 2759 (2000).